nature neuroscience

UNC-46 is required for trafficking of the vesicular GABA transporter

Kim Schuske, Mark T Palfreyman, Shigeki Watanabe & Erik M Jorgensen

Mutations in *unc-46* in *Caenorhabditis elegans* cause defects in all behaviors that are mediated by GABA. Here we show that UNC-46 is a sorting factor that localizes the vesicular GABA transporter to synaptic vesicles. The UNC-46 protein is related to the LAMP (lysosomal associated membrane protein) family of proteins and is localized at synapses. In *unc-46* mutants, the vesicular transporter is not found specifically in synaptic vesicles but rather is diffusely spread along the axon. Mislocalization of the transporter severely reduces the frequency of miniature currents, but the remaining currents are normal in amplitude. Because the number of synaptic vesicles is not depleted, it is likely that only a fraction of vesicles harbor the transporter in *unc-46* mutants. Our data indicate that the transporter and UNC-46 have mutual roles in sorting. The vesicular GABA transporter recruits UNC-46 to synaptic vesicle precursors in the cell body, and UNC-46 sorts the transporter at the cell body and during endocytosis at the synapse.

Neurotransmitters are produced in the cytoplasm and are loaded at high concentrations into synaptic vesicles by vesicular neurotransmitter transporters. For transporters to function correctly, they must be trafficked to the correct cellular compartment at the Golgi. For example, in PC12 cells the vesicular acetylcholine transporter (VAChT) is preferentially localized to small synaptic-like vesicles, whereas the vesicular monoamine transporter (VMAT) is localized to large, dense-core vesicles[1,2]. Negatively charged residues near the dileucine motif direct VMAT to dense-core vesicles. VAChT, which lacks these residues, can be directed to dense-core vesicles by substituting negatively charged amino acids at these positions[3]. Presumably, these residues interact with unidentified sorting factors that enable the transporters to be localized in one or the other compartment.

Similarly, at the synapse, transporters must be recovered from the plasma membrane after vesicle fusion and sorted back into synaptic vesicles. Recent data support the idea that clathrin is involved in the recycling of vesicular transporters. For example, endocytosis of the vesicular acetylcholine transporter is blocked by either mutation of the dileucine clathrin adaptor binding motif in the cytoplasmic tail of the transporter or depletion of free clathrin in cultured cells[4]. The vesicular glutamate transporter (VGLUT1) specifically interacts with the endocytosis protein endophilin, and this interaction is important for recycling of the transporter to synaptic vesicles under conditions of high-frequency stimulation[5–7]. It is not known what proteins are involved in sorting the vesicular GABA transporter to synaptic vesicles at either the Golgi or at the synapse.

Genetic studies of GABA neuron function in *Caenorhabditis elegans* have identified five genes that are required specifically for GABA neurotransmission[8]. Mutants that have defective inhibitory GABA neurotransmission show a hypercontracted muscle phenotype called a 'shrinker' phenotype. Molecular characterization of four of these five shrinker mutants identified the components of a functioning GABA synapse, including genes for GABA neuron identity (*unc-30*), GABA synthesis (*unc-25*), GABA transport (*unc-47*) and the inhibitory GABA receptor (*unc-49*)[9–12]. Of particular importance for this study is the *unc-47* gene, which encodes the vesicular GABA transporter (referred to as VGAT because glycine does not seem to be a primary neurotransmitter in invertebrates)[11]. Because the currently cloned genes cover all of the known fundamental requirements of a functioning GABA synapse, it seemed likely that the remaining gene, *unc-46*, might encode a protein with a novel role in GABA neurotransmission.

In this study we report the cloning and characterization of *unc-46*. The *unc-46* gene encodes a protein that functions with the VGAT transporter. UNC-46 is required primarily at the synapse to localize VGAT to synaptic vesicles. Conversely, VGAT is required to localize UNC-46 to synaptic vesicle precursors at the endoplasmic reticulum or Golgi.

RESULTS

UNC-46 is related to LAMP proteins

Like other members of the shrinker class of genes, *unc-46* mutants hypercontract when touched, and therefore lack the inhibitory actions of GABA. In addition, *unc-46* mutants miss enteric muscle contractions, which are controlled by an excitatory action of GABA (**Table 1**). The universal disruption of GABA function in *unc-46* mutants is not due to a defect in GABA synthesis, as assayed by GABA immunoreactivity[13]. *unc-46* was mapped to between *let-419* and *let-443* near the physical marker eP74. Cosmids in this interval were injected into mutant worms, and a single cosmid F55B10 rescued the *unc-46* mutant phenotype. Individual open reading frames within this genomic region

Howard Hughes Medical Institute and the Department of Biology, University of Utah, 257 South 1400 East, Salt Lake City, Utah 84112-0840, USA. Correspondence should be addressed to E.M.J. (jorgensen@biology.utah.edu).

Received 11 January; accepted 9 May; published online 10 June 2007; doi:10.1038/nn1920

Table 1 GABA-stimulated muscle contractions

	unc-46 (n2476)	unc-46 (e177)	unc-46 (e642)	unc-46 (e300)	unc-46 (e177); unc-46resc	unc-46 (e642); unc-470Ex
Enteric muscle contractions per defecation cycle	0.13	0.43	0.43	0.37	0.97	0.97

were amplified using polymerase chain reaction (PCR) and injected into *unc-46* mutants. A 4.2-kb PCR fragment containing the open reading frame C04F5.3 rescued the *unc-46* mutant phenotype (**Supplementary Fig. 1** online).

To confirm the gene identity of *unc-46*, we sequenced the three known *unc-46* alleles. In each allele, we found mutations in the C04F5.3 open reading frame (**Fig. 1** and **Supplementary Fig. 1**). Two of the alleles, *unc-46(e300)* and *unc-46(e177)*, are nonsense mutations that would lead to small truncated proteins and are therefore likely to be null alleles. The third allele, *e642*, is a mutation in the splice acceptor of exon 5 and its locomotory phenotype is identical to the other alleles.

We deduced the UNC-46 protein sequence from a 0.9-kb cDNA from C04F5.3. The UNC-46 protein is a type I transmembrane protein, 259 amino acids in length (**Fig. 1** and **Supplementary Fig. 2** online), that comprises a cleavable signal peptide, a single LAMP repeat containing several glycosylation sites, a transmembrane domain and a 25-amino-acid cytoplasmic tail. The sequence of the UNC-46 protein exhibits weak sequence homology, as well as a conserved predicted secondary structure, with the LAMP family of glycoproteins[14]. There are two bona fide LAMP proteins in *C. elegans* (LMP-1[15] and LMP-2), indicating that although UNC-46 is related to LAMP proteins, it is not likely to be the functional homolog of LAMP proteins in *C. elegans* (**Fig. 1** and **Supplementary Fig. 2**). UNC-46 is most similar to the predicted human protein C20orf103 and has homologs in mouse, rat, cow, chicken, *Xenopus* and zebrafish as well as several other nematodes, indicating that UNC-46 might be a member of a new subclass of evolutionarily conserved LAMP-related proteins. The mouse C20orf103, also known as BAD-LAMP, is highly expressed in the nervous system and in the neocortex of the postnatal brain (GFN SymAtlas, http://symatlas.gnf.org/SymAtlas/; Allen Brain Atlas, http://www.brain-map.org)[16–18]. Because the UNC-46 protein is related to LAMP proteins, and because the *unc-46* defect specifically eliminates GABA function, it is possible that UNC-46 is associated with an acidified compartment in GABA neurons.

unc-46 is expressed in GABA neurons

To determine in which cells *unc-46* is expressed, we placed green fluorescent protein (GFP) under the control of the *unc-46* promoter (*Punc-46:GFP*). *unc-46* is expressed in all 26 GABA neurons, as well as in a small number of unidentified neurons in the head, indicating that *unc-46* might have a role that is distinct from GABA function in these cells (**Fig. 2a**).

The UNC-30 transcription factor regulates expression of the genes for the biosynthetic enzyme glutamic acid decarboxylase (*unc-25*) and VGAT (*unc-47*) in the VD and DD motor neurons of *C. elegans*[13,19,20]. The *unc-46* gene is similarly regulated by UNC-30. *Punc-46:GFP* is not expressed in the VD and DD motor neurons in an *unc-30* mutant background (**Fig. 2b**).

UNC-46 is not required for GABA neuron development

UNC-30 also controls the morphology and synaptic connectivity of GABA neurons (J. White, personal communication), and *unc-46* might mediate these functions of *unc-30*. To assay neuronal architecture in *unc-46* mutants, we labeled GABA neurons using a GFP reporter under the control of the *unc-47* promoter. Axon morphology was normal in *unc-46* animals (**Supplementary Fig. 3** online). To determine whether synapses form in the *unc-46* mutants, we used GFP tags to analyze the distribution of the vesicle proteins synaptobrevin and synaptotagmin in GABA neurons. These proteins are localized to synaptic varicosities in wild-type animals[21,22]. The distribution of synapses marked by synaptobrevin in GABA motor neurons in *unc-46* mutants is similar to that of the wild type (**Fig. 2c**; in the dorsal cord, wild type 2.7 puncta per 10 μm, $n = 7$; *unc-46(e177)* 2.5 puncta per 10 μm, $n = 6$), indicating that the development of synapses is normal in these animals. Similarly, the distribution of synapses marked by synaptotagmin-GFP in GABA motor neurons (M. Gu and E.M.J., unpublished data) in *unc-46* mutants is the same as in the wild type (dorsal nerve cord, wild type 2.5 puncta per 10 μm, $n = 5$; *unc-46(e642)* 2.3 puncta per 10 μm, $n = 12$). The levels of synaptobrevin and synaptotagmin are also not decreased in *unc-46* mutants (synaptobrevin-GFP: wild type 55.0 ± 7.6, $n = 6$; *unc-46(e177)* 61.0 ± 5.3, $n = 7$; $P = 0.55$; synaptotagmin-GFP:

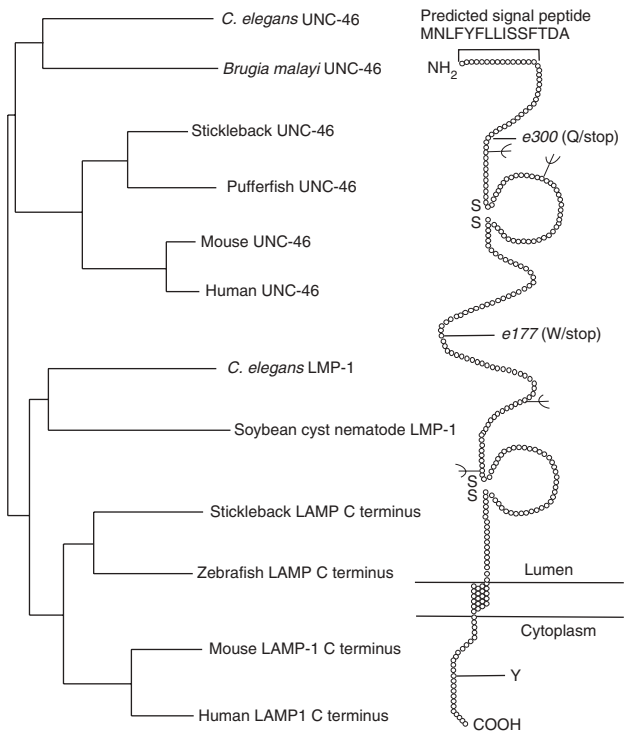

Figure 1 UNC-46 phylogenetic tree and predicted secondary structure. Left, the UNC-46 (C04F5.3) protein was aligned by ClustalX (**Supplementary Fig. 1**) and the phylogenetic tree determined by NJplot. The UNC-46 homologs from the nematodes *Brugia* and *Globodera* were not included in the tree as these sequences are partial. Right, the predicted secondary structure of UNC-46. UNC-46 contains a single LAMP repeat, which contains two cysteine loops, in contrast to bonafide LAMP proteins which contain two LAMP repeats and four cysteine loops. The positions of mutated amino acids are indicated. The *e300* and *e177* alleles are stop mutations; *e642* is a mutation of the splice acceptor site of exon five (not shown). All three alleles are EMS induced. Predicted *N*-linked (N35, N63, N146 and N166) glycosylation sites are indicated by branches.

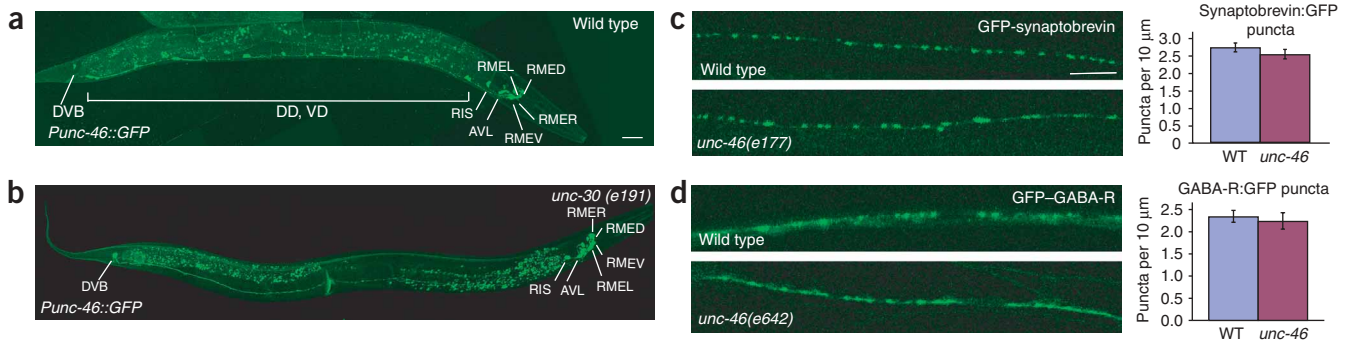

Figure 2 The *unc-46* gene is expressed in GABA neurons and is not required for neuron development. (**a**) Cellular expression of *unc-46*. GFP driven by the *unc-46* promoter is expressed in the 26 GABA neurons in wild-type worms. Two additional pairs of unidentified neurons in the head also express *unc-46*. (**b**) Expression of *unc-46* is regulated by the homeodomain transcription factor UNC-30. Expression of GFP driven by the *unc-46* promoter is absent in all ventral cord neurons (VD and DD) in *unc-30(e191)* mutants. However, head neurons AVL and RIS, the four RMEs and the unidentified neurons all express GFP in the absence of UNC-30, as does the tail neuron DVB. Scale bar, 30 µm. (**c**) GFP-tagged synaptobrevin, a synaptic vesicle protein, is localized to synapses in *unc-46* mutants. A region of the dorsal nerve cord at the reflex of the gonad was analyzed in adult wild-type and *unc-46(e177)* animals. The density of synaptobrevin-GFP puncta in *unc-46* mutants is the same as in the wild type (right). (**d**) A GFP-tagged GABA receptor is properly clustered in the body wall muscle of *unc-46* mutants. A region of the dorsal nerve cord at the reflex of the gonad was analyzed in adult wild-type and *unc-46(e642)* animals. The density of UNC-49–GFP puncta in *unc-46* animals is the same as in wild type animals (right). Scale bar, 10 µm.

wild type 30.7 ± 2.9, $n = 5$; *unc-46(e642)* 43.4 ± 2.5, $n = 12$; mean fluorescence ± s.e.m., $P = 0.01$). Occasionally, synaptobrevin and synaptotagmin puncta appear to be slightly more diffuse and variable in size in *unc-46* mutants. A similar phenotype is observed in the absence of VGAT, in *unc-47* mutants (data not shown), indicating that this defect is not specific to a loss of UNC-46. To determine whether the development of postsynaptic components is normal, we examined the distribution of a GFP-tagged GABA receptor (UNC-49) at neuromuscular junctions[12]. We confirmed that the number of and distance between postsynaptic receptor clusters is the same in *unc-46* mutants and as in wild-type animals (**Fig. 2d**; in the dorsal cord, wild type 2.3 ± 0.14 puncta per 10 µm; *unc-46(e642)* 2.2 ± 0.19 puncta per 10 µm; $n = 6$ each). Thus, the number of pre- and postsynaptic puncta appear to be similar in *unc-46* mutant animals and in wild-type animals, indicating that synaptic development is normal and that the mutant animals are instead likely to be defective for GABA neurotransmission.

UNC-46 is localized to synapses

To determine the subcellular distribution of UNC-46 protein, we inserted GFP at the amino terminus of UNC-46 after the signal peptide. The construct rescues *unc-46* mutants, showing that the fusion protein is localized and functional. UNC-46–GFP is primarily localized to synaptic varicosities in the dorsal and ventral cord (**Fig. 3a**). Synaptic vesicle proteins, including VGAT, require the synaptic vesicle kinesin UNC-104 for localization to synapses[11,22]. In *unc-104* mutants, UNC-46–GFP is mislocalized to the cell bodies (**Fig. 3b**). This mislocalization indicates that UNC-46, like VGAT, is delivered to the synapse by synaptic vesicle precursors.

VGAT is required to transport UNC-46 to synapses

To determine whether the expression or localization of UNC-46 depends on the other GABA-specific proteins GAD or VGAT, we crossed UNC-46–GFP into *unc-25* and *unc-47* mutant strains. Both strains also lacked the *unc-46* gene so that there would not be

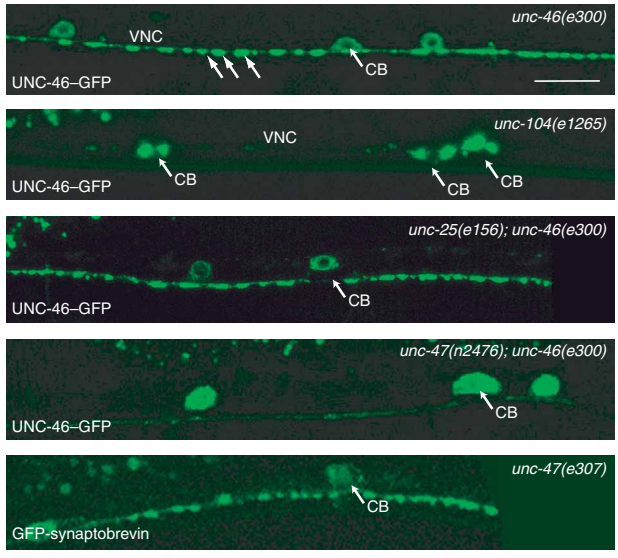

Figure 3 UNC-46 is localized at synapses. (**a**) UNC-46–GFP is localized to varicosities corresponding to neuromuscular synapses (arrows) of the VD motor neurons in the ventral nerve cord (VNC); some fluorescence can be seen in the cell body (CB). (**b**) UNC-46–GFP is not transported to synapses in a mutant lacking the kinesin dedicated to synaptic vesicles (*unc-104(e1265)*), but rather is mislocalized to a perinuclear compartment in the cell body. (**c**) UNC-46–GFP is localized at synapses in *unc-25(e156)* mutants with no decrease in fluorescence intensity of GFP (*unc-46(e300); GFP:UNC-46*: 78.9 ± 5.0, $n = 7$; *unc-25(e156); unc-46(e300); GFP:UNC-46*: 76.5 ± 9.2, $n = 8$; $P = 0.83$). (**d**) UNC-46–GFP is mislocalized to the motor neuron cell body in *unc-47* mutants. The UNC-46–GFP protein accumulates in a reticulated compartment, possibly the endoplasmic reticulum or Golgi, in the cell body. Very weak UNC-46–GFP expression can be seen in ventral cord axons only when the laser on the confocal microscope is set so that the puncta in the control animals are significantly overexposed. There is at least a 74% reduction in average fluorescence intensity of UNC-46–GFP in the ventral nerve cord of *unc-47* mutants relative to control (average fluorescence intensity ± s.e.m.: *unc-47(n2476); unc-46(e300); oxIs103[UNC-46:GFP]* 19.1 ± 0.8, $n = 5$; *unc-46(e300); oxIs103* 73.9 ± 2.2, $n = 4$; $P < 0.0001$, two-tailed *t*-test). (**e**) GFP-synaptobrevin is localized to synapses in *unc-47(e307)*. Scale bar, 10 µm. All images are of GABA neurons from the ventral nerve cord of adult hermaphrodites.

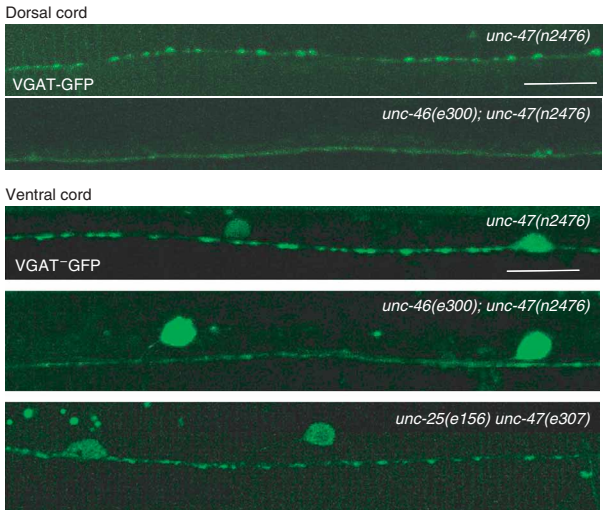

Figure 4 Localization of VGAT in *unc-46* and *unc-25* mutants. (**a**) Dorsal nerve cord. VGAT-GFP is diffusely localized in nerve cords of *unc-46* mutants. VGAT-GFP was expressed in an *unc-47(n2476)* strain so that the endogenous protein would not compete with the GFP-tagged version. (**b**) Ventral nerve cord. Top, VGAT-GFP accumulates at synaptic puncta in the ventral cord of wild-type animals. Middle, VGAT-GFP is diffuse in the ventral cord and protein accumulates in the cell body in *unc-46* mutants (genotype *unc-47(n2476); unc-46(e300)*). There is a 18% reduction in average fluorescence intensity in the ventral nerve cord of *unc-46* mutants relative to control (average fluorescence intensity ± s.e.m.: *unc-47(n2476); unc-46(e300); oxIs102[UNC-47:GFP]*: 26.3 ± 1.77, $n = 5$; *unc-47(n2476); oxIs102* 32.1 ± 3.89, $n = 5$; $P = 0.21$, two-tailed *t*-test). Below, VGAT-GFP is localized at synapses in *unc-25(e156)* mutants and there is no significant decrease in the average fluorescence intensity of GFP in these animals (*unc-47(e307); UNC-47:GFP*: 25.0 ± 3.3, $n = 7$; *unc-25(e156) unc-47(e307); UNC-47:GFP*: 20.5 ± 1.7, $n = 6$; $P = 0.28$). Scale bar, 10 μm.

competition between the tagged protein and the endogenous protein. Interestingly, although the expression and localization of UNC-46 are normal in the absence of GAD, UNC-46 requires VGAT to be localized to synapses (**Fig. 3c**,**d**). In *unc-47* mutants, UNC-46 was almost absent from the dorsal and ventral nerve cords, but was present at high levels in a diffuse compartment in the cell body. Specifically, there is at least a 74% decrease in axonal GFP in *unc-47* mutants as compared to control animals (**Fig. 3c**,**d** and see Methods). The defect in UNC-46 protein transport in *unc-47* mutants is not caused by a defect in transport of vesicles to the synapse, as synaptic vesicle components are generated and transported normally in these mutants (**Fig. 3e**). Therefore, localization of UNC-46 to synaptic vesicles precursors requires the vesicular GABA transporter. These data indicate that UNC-46 and VGAT could be functionally associated. There are two possible functions for UNC-46 in GABA loading: UNC-46 could be required for VGAT trafficking, or as an accessory subunit of VGAT.

UNC-46 is required to localize UNC-47 to synapses

To determine whether UNC-46 is required to localize the vesicular GABA transporter to synaptic vesicles, a construct containing a GFP-tagged VGAT was crossed into *unc-46* mutants. The tagged VGAT rescues the *unc-47* shrinker and defecation defects; therefore, the tagged protein is properly localized and is functional. VGAT-GFP is seem in the cell bodies and at synaptic varicosities along the dorsal and ventral nerve cords (**Fig. 4a**,**b**). By contrast, in *unc-46* mutants, the GABA transporter is diffuse along the dorsal and ventral cords rather than concentrated in clusters of synaptic vesicles at synapses (**Fig. 4a**,**b**). The diffuse localization of VGAT-GFP in *unc-46* mutants was shown to be significant in a blind test (Fisher's exact test, $P = 0.0001$). The diffuse staining along axons in the *unc-46(e300)* mutants is accompanied by a measurable but not significant decrease in axonal fluorescence (82% of wild type), and a 1.7-fold increase in cell body fluorescence, showing that there is also a trafficking defect from the cell body. The mislocalization of VGAT is not simply due to a lack of GABA in synaptic vesicles. In GAD/*unc-25* mutants, there is no change in either the localization or levels of VGAT-GFP (**Fig. 4b**).

Vesicle numbers are normal in *unc-46* mutants

As VGAT seems to be mislocalized to the plasma membrane in *unc-46* mutants, it is possible that UNC-46 is required for synaptic vesicle endocytosis. To analyze the distribution of synaptic vesicles at synapses in *unc-46* mutants, we fixed worms using a high-pressure freezing protocol. A segment of the ventral nerve cord was reconstructed from serial electron micrographs and synaptic vesicles were quantified at GABA neuromuscular junctions. There are approximately the same number of synaptic vesicles at *unc-46* mutant synapses as at wild-type synapses (**Fig. 5a**). In addition, the number of docked vesicles is similar between *unc-46* mutants and wild-type animals (**Fig. 5b**).

Although the number of synaptic vesicles is similar between *unc-46* mutants and wild-type animals, *unc-46* mutants have a population of large vesicles at GABA synapses (**Fig. 5c–e**). Around 8% of the vesicles in *unc-46* mutants are large (defined as clear vesicles greater than 40 nm in diameter) whereas only 0.7% are large in the wild type. Most of these vesicles are found more than 350 nm from the dense projection. A similar result was obtained using a standard ice-cold glutaraldehyde fixation protocol and with a second allele *unc-46(e177)* (data not shown). Abnormal membranous structures have been observed in mouse neurons lacking the vesicular glutamate transporter, indicating that fusion of vesicles lacking neurotransmitter might disrupt membrane trafficking[23]. To determine whether the accumulation of large vesicles is due to a specific loss of *unc-46* or to a loss of GABA neurotransmission, we analyzed synaptic vesicle size in mutants defective for biosynthesis (*unc-25*) or transport of GABA (*unc-47*). In both mutants, we saw a significant population of large vesicles (*unc-25(e156)* 5% and *unc-47(n2476)* 3%) in GABA synapses but not in acetylcholine synapses (**Fig. 5d**,**e**). These data indicate that although membrane trafficking might be disrupted in *unc-46* mutants, this phenotype is common to all mutants with defects in GABA loading. Thus, electron microscopy shows no specific defect in synaptic vesicle endocytosis in *unc-46* mutants.

GABA release is defective in *unc-46* mutants

If VGAT is not properly localized to synaptic vesicles in *unc-46* mutants, then GABA synapses should show a decrease in miniature inhibitory postsynaptic currents. We recorded currents at GABA neuromuscular junctions using voltage-clamp recordings from body muscle cells (**Fig. 6a**). By blocking the ionotropic acetylcholine receptor with D-tubocurare, it is possible to isolate GABA-mediated responses in the muscle[24]. The frequency of GABA miniature post-synaptic currents ('minis') was reduced by 90% in *unc-46* mutants compared to wild-type animals (**Fig. 6b**). However, the miniature current rate in *unc-46* mutants was still greater than in animals lacking VGAT (*unc-47*), in which we recorded no GABA minis. The residual release of GABA in *unc-46* animals is consistent with the less severe behavioral phenotype observed in *unc-46* than in *unc-47* mutants (**Table 1**). There is no decrease in the mini amplitude for the few minis that remain in *unc-46* animals (**Fig. 6c**); therefore, some vesicles seem to be normally loaded

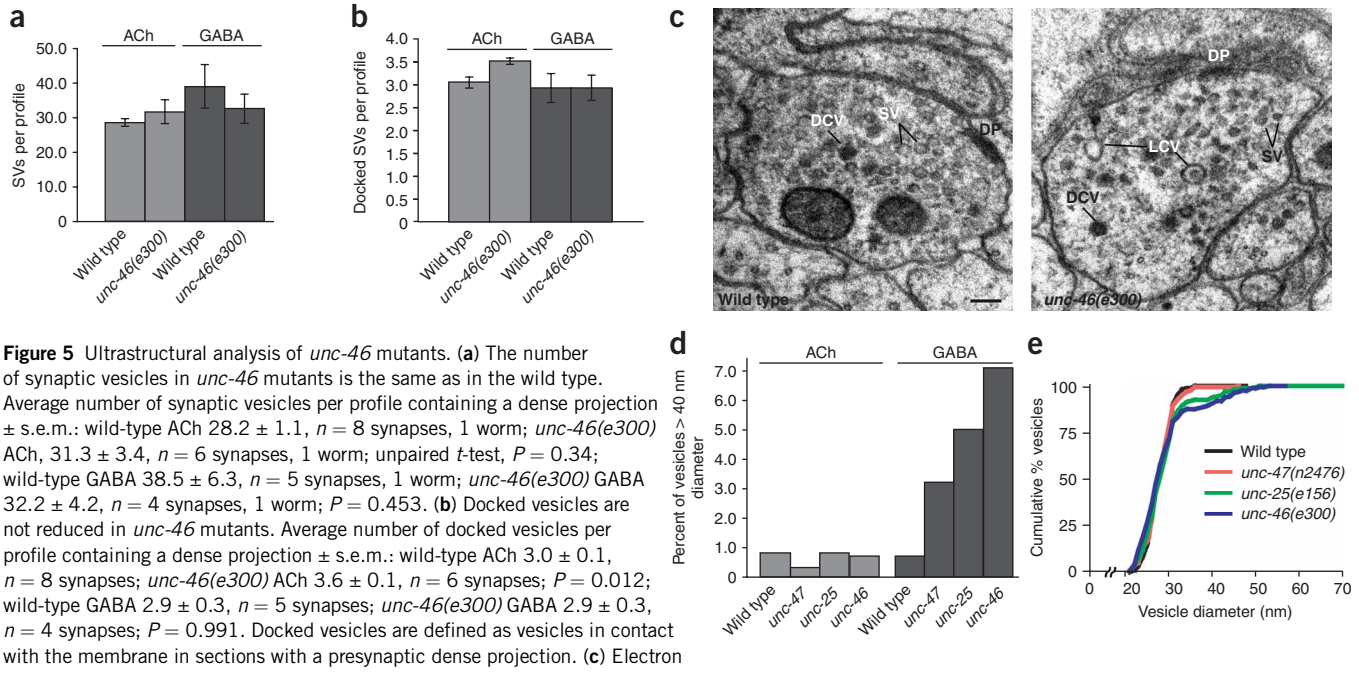

Figure 5 Ultrastructural analysis of *unc-46* mutants. (**a**) The number of synaptic vesicles in *unc-46* mutants is the same as in the wild type. Average number of synaptic vesicles per profile containing a dense projection ± s.e.m.: wild-type ACh 28.2 ± 1.1, $n = 8$ synapses, 1 worm; *unc-46(e300)* ACh, 31.3 ± 3.4, $n = 6$ synapses, 1 worm; unpaired *t*-test, $P = 0.34$; wild-type GABA 38.5 ± 6.3, $n = 5$ synapses, 1 worm; *unc-46(e300)* GABA 32.2 ± 4.2, $n = 4$ synapses, 1 worm; $P = 0.453$. (**b**) Docked vesicles are not reduced in *unc-46* mutants. Average number of docked vesicles per profile containing a dense projection ± s.e.m.: wild-type ACh 3.0 ± 0.1, $n = 8$ synapses; *unc-46(e300)* ACh 3.6 ± 0.1, $n = 6$ synapses; $P = 0.012$; wild-type GABA 2.9 ± 0.3, $n = 5$ synapses; *unc-46(e300)* GABA 2.9 ± 0.3, $n = 4$ synapses; $P = 0.991$. Docked vesicles are defined as vesicles in contact with the membrane in sections with a presynaptic dense projection. (**c**) Electron micrographs of GABA neuromuscular junctions. DP, presynaptic dense projection; LCV, large clear vesicle (> 40 nm); DCV, large electron-dense vesicle (~40 nm); SV, synaptic vesicle (~30 nm). Scale bar, 100 nm. (**d**) Synaptic vesicle diameters are normal, but large clear vesicles accumulate in GABA neurons in *unc-47(n2476)*, *unc-25(e156)* and *unc-46(e300)* mutants. (**e**) Cumulative plot of vesicle diameters from GABA neurons of wild-type, *unc-46*, *unc-25* and *unc-47* animals.

with GABA in the absence of *unc-46*. Although it is not statistically significant, there is a trend toward larger miniature currents in *unc-46* mutants which might indicate that the large vesicles that were observed using electron microscopy can fuse. These data are consistent with a defect in the loading of neurotransmitter into most synaptic vesicles at GABA neuromuscular junctions.

The ultrastructural data indicate that there is no decrease in the number of synaptic vesicles in GABA terminals or docked at the plasma membrane in *unc-46* mutants. The electrophysiological data show that there is a 90% reduction in GABA minis in *unc-46* mutants. The presence of rare minis indicate that occasional vesicles can be filled with GABA in the absence of *unc-46*. Thus, we can conclude that some GABA transporters are localized to vesicles and can function in the absence of UNC-46. Together, these data indicate that UNC-46 sorts VGAT into mature synaptic vesicles.

VGAT overexpression rescues *unc-46*

If the main function of UNC-46 is to localize VGAT, then overexpression of the transporter might compensate for mislocalization. We injected the genomic rescuing fragment of *unc-47* into *unc-46* mutants to generate high-copy arrays of the transporter gene. Using video tracking analysis (J. White and E.M.J., unpublished data), we found that transgenic *unc-46* mutants were significantly rescued for the locomotory defects (**Fig. 7**). *unc-47* and *unc-46* mutants move half as

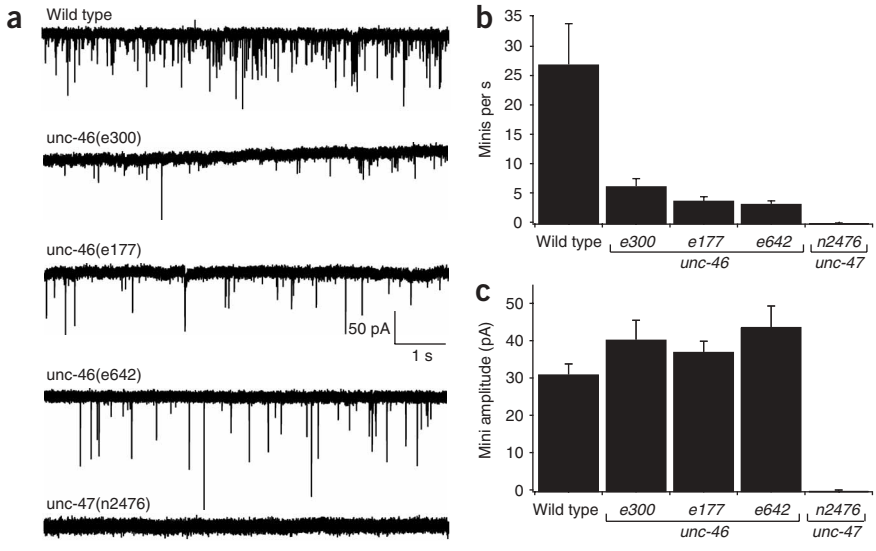

Figure 6 Electrophysiological analysis of *unc-46* mutants. (**a**) Representative traces from wild-type, *unc-46* and *unc-47* animals recorded in the presence of D-tubocurare (1 mM). (**b**) The frequency of minis is reduced by 90% in *unc-46* mutants (*e300* 6.5 ± 1.3 quanta s^{-1}, $n = 8$; *e177* 4.0 ± 0.7 quanta s^{-1}, $n = 7$; *e642* 3.5 ± 0.5 quanta s^{-1}, $n = 7$) compared to wild-type animals (27.3 ± 7.0 quanta s^{-1}, $n = 6$) (*e300* $P = 0.0054$, *e177* $P = 0.0041$, *e642* $P = 0.0035$). Minis are absent in *unc-47* mutants (*n2476* 0 ± 0 quanta s^{-1}, $n = 9$). (**c**) The amplitudes of the remaining minis are normal in *unc-46* mutants (*e300* 40.9 ± 5.2 pA, $n = 8$; *e177* 37.6 ± 2.9 pA, $n = 7$; *e642* 44.3 ± 5.6 pA, $n = 7$), compared to those of wild-type animals (31.6 ± 2.8 pA, $n = 6$) (*e300* $P = 0.1788$, *e177* $P = 0.1659$, *e642* $P = 0.0820$).

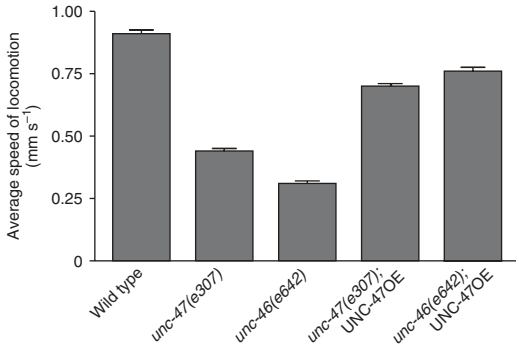

Figure 7 Locomotion of *unc-46* mutants is rescued by overexpression of VGAT. Average speed for each genotype is shown (wild type: 0.91 ± 0.01 mm s^{-1}, $n = 4$; *unc-47(e307)*: 0.4 ± 0.01 mm s^{-1}, $n = 4$; *unc-46(e642)*: 0.3 ± 0.01 mm s^{-1}, $n = 4$; *unc-47(e307);overexpressed UNC-47*: 0.7 ± 0.01 mm s^{-1}, $n = 4$; *unc-46(e642);overexpressed UNC-47*: 0.8 ± 0.02 mm s^{-1}, $n = 4$).

fast as the wild type (0.4, 0.3 or 0.9 mm s^{-1}, respectively). *unc-46* mutants that overexpress VGAT move at a similar velocity to wild-type worms (0.8 mm s^{-1}). Moreover, enteric muscle contractions are rescued in *unc-46* mutants by the presence of the *unc-47* extrachromosomal array (**Table 1**). These data indicate that, in the absence of UNC-46, the vesicular GABA transporter is mislocalized; but if the transporter is overexpressed, sufficient amounts of the protein will be on synaptic vesicles to fulfil its function.

DISCUSSION

Mutations in *unc-46* cause defects in GABA neurotransmission in *C. elegans*[13]. We have shown that UNC-46 is required for trafficking of the vesicular GABA transporter to synaptic vesicles. First, UNC-46 is expressed in GABA neurons and is localized to synapses. Second, in *unc-46* mutants, VGAT is not localized to synaptic vesicles but rather is diffusely localized along axons in synaptic regions. Third, in the absence of VGAT, UNC-46 is not localized at synapses and instead accumulates in cell bodies, indicating that a mutual relationship exists between the two proteins. Fourth, GABA miniature currents are reduced to 10% of their normal frequency in electrophysiological recordings from mutants, but mini amplitude is not decreased, consistent with a small population of vesicles being fully filled in the absence of UNC-46. Finally, overexpression of VGAT rescues the defects in *unc-46* mutants, underscoring the role of UNC-46 in trafficking of VGAT.

Ultrastructural studies show that vesicle numbers are normal at *unc-46* synapses, indicating that there is no gross defect in membrane endocytosis. Although we cannot rule out a role for UNC-46 in membrane endocytosis, it is generally believed that the machinery for endocytosis is shared by all neurons. By contrast, vesicle components that are unique to specific neurotransmitters should require specific recycling mechanisms, so the presence of a specific recycling factor for the GABA transporter is perhaps not surprising. In addition, loss of GABA exocytosis seems to have a slight but interesting indirect effect on membrane trafficking. In *unc-46*, *unc-25* (GAD) and *unc-47* (VGAT) mutants, there is a small increase in a population of large vesicles. Interestingly, abnormal membrane structures have been observed in mouse neurons lacking the vesicular glutamate transporter[23]. Together, these data indicate that in the absence of vesicle filling, membrane trafficking is altered. Two issues bear further discussion: first, what is the mechanism of UNC-46 action; and second, in which cellular compartment does UNC-46 act?

The uncoordinated phenotype of *unc-46* mutants can be attributed to a failure to localize VGAT. What does the structure of UNC-46 suggest about the potential mechanisms of its action? UNC-46 possesses a single LAMP repeat and is therefore distantly related to LAMP family proteins. LAMPs are among the most abundant membrane proteins on the surface of the lysosome[25] and might be required for the biogenesis of lysosomes and to protect the lysosomal membranes from hydrolytic enzymes[14]. Surprisingly, mice lacking both LAMP-1 and LAMP-2 still contain lysosomes but there are trafficking defects in these organelles[26,27]. The mutants also accumulate abnormally high levels of cholesterol in late endosomes[26,27]; and the mannose-6 phosphate receptor is mislocalized to perinuclear vesicles[28]. One possibility is that the changes in lipid composition cause the mislocalization of the mannose-6 phosphate receptor. Alternatively, the LAMP proteins might act as sorting factors. LAMP proteins have short cytoplasmic tails that direct the proteins, and perhaps associated proteins, into vesicles bound for the lysosome[29]. It is possible that UNC-46 and LAMP proteins function in a similar manner to sort proteins to acidified compartments.

Although UNC-46 could have a secondary role as a functional subunit of VGAT, there are several reasons to believe that it is not required as an auxiliary subunit for the GABA transporter. First, the primary defect in *unc-46* mutants is whether a vesicle contains any neurotransmitter, not how much neurotransmitter is in a vesicle. In *unc-46* mutants, only a few synaptic vesicles are fully loaded with neurotransmitter; thus, most vesicles lack a functional transporter, but some vesicles seem to bear at least one copy of the transporter. One copy might be enough: experiments in *Drosophila* indicate that one transporter is sufficient to fully load a synaptic vesicle[30]. Second, the fact that some vesicles are filled with neurotransmitter shows that VGAT can fill a vesicle to normal levels in the absence of the putative UNC-46 'auxiliary' subunit. Third, when VGAT is overexpressed in an *unc-46* mutant, the *unc-46* uncoordination and defecation defects are rescued. These results indicate that the defect in *unc-46* mutants is not a failure of the transporter to function but is rather a failure to get the transporter to the right place.

At which trafficking step does UNC-46 act? In the simplest model, UNC-46 is required to sort VGAT into synaptic vesicle precursors at the Golgi. Indeed, in the absence of UNC-46, VGAT accumulates in the cell body, indicating that UNC-46 is involved in VGAT transport in the cell body. However, the transporter is still translocated to distal regions of the axon; there is only an 18% decrease in the amount of GFP-tagged VGAT in *unc-46* mutant axons. Nevertheless, the transporter is not being swept up and concentrated into synaptic puncta by the synaptic vesicle endocytic machinery — it remains diffuse even in synaptic regions. Thus, UNC-46 seems also to contribute to the retrieval of VGAT at the synapse. Within the synapse, UNC-46 could sort VGAT from the plasma membrane, or from a transient endosomal compartment. Although a sorting endosome is not observed at *C. elegans* synapses, large-diameter cisternae can be observed in strains with trafficking defects, such as in synaptojanin, endophilin and AP180 mutants[31–33]. These large cisternae might represent a transient sorting compartment that has been stabilized by disruption of endocytosis. Interestingly, the closest vertebrate homolog of UNC-46, BAD-LAMP, seems to be highly expressed in the neocortex of the postnatal mouse brain[16]. The protein shuttles between the plasma membrane and an unidentified early endosomal compartment. The compartmental localization seems to rely on interactions with dynamin and the clathrin adaptor AP2, as inhibition of these proteins in cultured cells disrupts the internalization process. Therefore, this new family of LAMP-like proteins might define an unidentified sorting compartment.

In conclusion, these data support a model in which two trafficking steps are required for the generation of functional synaptic vesicles in GABA neurons. In the cell body, VGAT is sorted to synaptic vesicle precursors and recruits UNC-46 to these vesicles (**Supplementary Fig. 4** online). At the synapse, UNC-46 recruits VGAT to synaptic vesicles during endocytosis. These results indicate that the mechanisms for sorting synaptic vesicle components at the Golgi differ from those at the synapse.

METHODS

***C. elegans* strains.** The wild strain is Bristol N2. All mutants used for phenotypic analyses were outcrossed at least twice. These strains are EG1298: *unc-46(e177)*, EG1098: *unc-46(e300)*, EG2985: *unc-46(e642)* and EG1141: *unc-47(n2476)*. The strains used for microinjections were: EG1137: *unc-46(e642); lin-15(n765ts)* and EG1578: *unc-46(e177); lin-15(n765ts)*. The *unc-46* rescued strain is EG1663: *unc-46(e177); oxEx248*[pKS1.10]. GFP-expressing strains are: EG1667: *oxEx249[Punc-46:GFP, lin-15+]; lin-15(n765ts)*, EG3493: *oxEx249[Punc-46:GFP, lin-15+]; unc-30(e191)*, EG3252: *unc-47(n2476); lin-15(n765ts) oxIs102[UNC-47:GFP, lin-15+]*, EG1827: *unc-46(e300); lin-15(n765ts) oxIs103[UNC-46:GFP, lin-15+]*, EG3434: *unc-47(n2476); unc-46(e300), oxIs102*, EG3435: *unc-47(n2476); unc-46(e300); oxIs103*, EG1827: *unc-104(e1265); oxEx250[UNC-46:GFP, lin-15+]*, EG4559: *unc-47(e307 unc-25(e156); oxxIs102*, EG4560: *unc-25(e156); unc-46(e300); oxIs103*. The synaptobrevin (VAMP)-GFP strains are: EG3148: *unc-46(e177); lin-15(n765ts) nIs52[VAMP:GFP, lin-15+]*, EG1036: *unc-47(e307); nIs52 [VAMP:GFP, lin-15+] lin-15(n765ts)*. The synaptotagmin-GFP strains are: EG3855: *oxIs224[Punc-47:GFP::SNT-1, lin-15+]; lin-15(n765ts)* and EG4557: *unc-46(e642); oxIs224*. The GABA receptor UNC-49–GFP strains are, EG1653: *oxIs22[UNC-49:GFP, lin-15+]; lin-15(n765ts)* and EG2936: *unc-46(e642); oxIs22 lin-15(n765ts)*. The VGAT overexpression strain is EG1138: *unc-46(e642); oxEx655[unc-47 5.2kb genomic rescue, lin-15+]; lin-15(n765ts)* and EG1139: *unc-46(e642); oxEx656[unc-47 5.2kb genomic rescue, lin-15+]; lin-15(n765)*.

Rescue of *unc-46* mutants. For rescue of *unc-46* mutants, we injected a pool of cosmids near the polymorphism eP74; ZK702, T25H12, C16F1 and F55B10 at a concentration of 20 ng μl^{-1}, for each cosmid, together with 60 ng μl^{-1} of *lin-15+* DNA (EK L15[34]) into *unc-46 (e642); lin-15(n765ts)* worms. Subsequently, individual cosmids were injected at a concentration of 20 ng μl^{-1}, and only one, F55B10, rescued the *unc-46* mutant phenotype A 4.2-kb PCR fragment was amplified using the primers: 5′-ATACTTATTTTCCTAATGGT CAAG-3′ and 5′-TTTTGAAATGAACTGTTAGAAGGAGG-3′, which contains 1.3 kb of sequence upstream of the start codon and 1.3 kb downstream of the stop codon. This fragment contains a single complete open reading frame corresponding to C04F5.3 and rescued the *unc-46* mutant phenotype. The rescuing fragment was TA cloned into the pCR2.1 vector (Invitrogen). This plasmid pKS1.10 was injected into *lin-15(n765ts); unc-46(e177)* mutants and also rescued the mutant phenotypes.

For the overexpression of *unc-47* in an *unc-46* mutant, we injected ~30 ng μl^{-1} of Bluescript vector containing a 5.2-kb *Bam*HI *unc-47* genomic DNA fragment (pKS8.1) together with 60 ng μl^{-1} of EK L15 (lin-15+) DNA into *lin-15(n765ts); unc-46(e642)* worms. We obtained two arrays, *oxEx655* and *oxEx656*, that were rescued for the *unc-46* mutant phenotype.

cDNA identification and sequence. A cDNA, yk541d11, corresponding to the C04F5.3 open reading frame was obtained from the collection of cDNAs isolated by Y. Kohara (http://nematode.lab.nig.ac.jp/dbest/keysrch.html; accession number, 17557625). We used Prosite and NetOGlyc computer prediction programs to prediced N- (N35, N63, N146, and N166) and O- (T17, T18, S19, T20) linked glycosylation sites.

***unc-46*::GFP expression constructs.** The *unc-46* promoter expression construct, pKS2.15, was constructed using the GFP and *unc-54* terminator sequence contained in pPD95.85. The GFP sequence was amplified with primers containing *Pin*AI sites on both sides. The *Pin*AI sites were engineered so that they were in frame to the endogenous *Pin*AI site within the first exon of the *unc-46* gene and contained the ATG start codon from GFP. The amplified GFP and *unc-54* terminator was cloned into the *Pin*AI site in the full-length rescuing subclone for *unc-46*. A GFP product should be produced that is fused with 24 amino acids of UNC-46 protein at the N terminus. pKS2.15 was injected into *lin-15(n765ts)* worms at a concentration of 25 ng μl^{-1} along with EK L15 (60 ng μl^{-1}). We obtained five lines that contained the u46GFPntx construct, and the analyzed array is *oxEx249*.

To construct a GFP-tagged version of UNC-46, we PCR-amplified GFP such that it was flanked by *Pin*AI restriction sites. This GFP fragment was subcloned into an endogenous *Pin*AI site in exon 1 of the rescuing fragment for the *unc-46* gene. This construct, pKS9.1, generates an UNC-46 protein with an insertion of GFP after amino acid 24. pKS9.1 was injected into *unc-46(e117); lin-15(n765ts)* hermaphrodites, at a concentration of 30 ng μl^{-1} and coinjected with EK L15 at a concentration of 60 ng μl^{-1} . The U46GFPntl construct rescued the *unc-46* mutant phenotype, and the integrated array is *oxIs103*.

Quantitative fluorescence microscopy. We collected images using a 63× objective on a Zeiss Pascal Confocal microscope. Animals were immobilized with 2% phenoxypropanol and rotated so that their ventral cords were facing up. The same region of the cord, anterior of the vulva, was imaged. All images were taken using the same settings on the same day after the laser was allowed to stabilize for 30 min. Maximum intensity projections were analyzed using Image J software. The ventral cord was outlined for each animal and the average fluorescent value was calculated. The average fluorescent values were then averaged over five worms for both the control (*unc-47(n2476); oxIs102[UNC-47:GFP]*) and experimental (*unc-47(n2476); unc-46(e300), oxIs102[UNC-47:GFP]*) strains. For the *unc-46(e300); oxIs103[UNC-46:GFP]* and *unc-47(n2476); unc-46(e300); oxIs103[UNC-46:GFP]* strains, images were taken at a laser intensity high enough that the nerve cord was visible in the *unc-47* mutant background. Because of this, the UNC-46–GFP often reached maximum pixel intensity in the *unc-46* control background, making it difficult to determine the absolute difference in protein levels between *unc-47* mutants and control animals. The 74% reduction of UNC-46 in axons is therefore a minimum value. **Figures 3** and **4** show examples of images that were analyzed.

Electrophysiology. Electrophysiolgical methods were performed as described[24,35] with minor adjustments. Briefly, the animals were immobilized in cyanoacrylic glue (B. Braun, Aesculap) and a lateral incision was made to expose the ventral medial body wall muscles. The preparation was then treated with collagenase (type IV; Sigma) for 15 s at a concentration of 0.5 mg ml^{-1}. The muscle was then voltage clamped using the whole-cell configuration at a holding potential of –60 mV. GABA minis were isolated by blocking cholinergic currents with 1 mM D-tubocurare (Sigma) from a perfusion system. All recordings were made at room temperature (21 °C) using an EPC-9 patch-clamp amplifier (HEKA) run on an ITC-16 interface (Instrutech). Data were acquired using Pulse software (HEKA).

The extracellular solution contained: 150 mM NaCl, 5 mM KCl, 5 mM $CaCl_2$, 1 mM $MgCl_2$, 10 mM glucose, 15 mM Hepes, pH 7.35 and sucrose to 340 mOsm. The pipet solution contained: 120 mM KCl, 20 mM KOH, 4 mM $MgCl_2$, 5 mM *N*-Tris (hydroxdymethyl) methyl-2-aminoethane-sulfonic acid, 0.25 mM $CaCl_2$, 4 mM NaATP, 36 mM sucrose, 5 mM EGTA, pH 7.2 and sucrose to 335 mOsm. All data analysis and graph preparation was performed using Pulsefit (HEKA), Mini Analysis (Synaptosoft) and Igor Pro (Wavemetrics).

Electron microscopy. Wild-type (N2), *unc-46(e300), unc-47(n2476)* and *unc-25(e156)* adult nematodes were prepared in parallel for transmission electron microscopy as described[36]. Briefly, 10 animals that were raised at room temperature were placed onto a freeze chamber (100-µm well of type A specimen carrier) containing space-filling bacteria, covered with a type B specimen carrier flat side down, and frozen instantaneously in the BAL-TEC HPM 010. The frozen animals were fixed in Leica EM AFS system with 0.5% glutaraldehyde and 0.1% tannic acid in anhydrous acetone for 4 days at –90 °C, followed by 2% osmium tetroxide in anhydrous acetone for 38.9 h with gradual temperature increase (constant temperature at –90 °C for 7 h, then increase by 5 °C per h to –25 °C over 13 h, constant temperature at –25 °C for 16 h, and then increase by 10 °C per h to 4 °C over 2.9 h). The fixed animals were embedded in araldite resin following the infiltration series (30% araldite/acetone for 4 h, 70% araldite/acetone for 5 h, 90% araldite/acetone overnight,

and pure araldite for 8 h). Mutant and control blocks were blinded. Ribbons of ultrathin (33 nm) serial sections were collected using an Ultracut E microtome. Images were obtained on a Hitachi H-7100 electron microscope using a Gatan slow scan digital camera. We cut 250 ultrathin contiguous sections and reconstructed the ventral nerve cord from one animal representing each genotype. We analyzed images using Image J software. We counted the number of synaptic vesicles ($\sim$30 nm), dense-core vesicles ($\sim$40 nm) and large vesicles ($>$40 nm) in each synapse, and measured their distance from presynaptic specializations and the plasma membrane as well as the diameter of each, in cholinergic neurons VA and VB and the GABA neuron VD. The average number of synaptic vesicles and docked vesicles per profile were calculated for each set of images containing a part of the presynaptic dense projection. The numbers for each profile were averaged to obtain the final value.

Worm tracking. We placed single worms of each genotype in a 5-µl drop of M9 on a plate containing 0.02% bromophenol blue for contrast. Four worms were tested for each strain on a single plate. We made 10-min movies after evaporation of the M9. We analyzed the data using a program created by J. White that calculates the distance traveled every second.

Note: Supplementary Information is available on the Nature Neuroscience website.

ACKNOWLEDGMENTS

We thank J. White for use of his worm tracking system, M. Gu for the GFP-tagged synaptotagmin strain, the *C .elegans* Genome Center for strains, the Sanger Center for cosmids, Y. Kohara for the *unc-46* cDNA, J. Shine for *unc-46* mapping data, J. Thomas for the *Brugia* gene prediction, and D. Joshi and J. Huang for technical assistance.

AUTHOR CONTRIBUTIONS

M.T.P. performed the electrophysiology experiments, S.W. performed the electron microscopy experiments and K.S. performed all other experiments and wrote the paper with E.M.J. and with help from M.T.P.

COMPETING INTERESTS STATEMENT

The authors declare no competing financial interests.

Published online at http://www.nature.com/natureneuroscience
Reprints and permissions information is available online at http://npg.nature.com/reprintsandpermissions

1. Liu, Y. *et al.* Preferential localization of a vesicular monoamine transporter to dense core vesicles in PC12 cells. *J. Cell Biol.* **127**, 1419–1433 (1994).
2. Liu, Y. & Edwards, R.H. Differential localization of vesicular acetylcholine and monoamine transporters in PC12 cells but not CHO cells. *J. Cell Biol.* **139**, 907–916 (1997).
3. Krantz, D.E. *et al.* A phosphorylation site regulates sorting of the vesicular acetylcholine transporter to dense core vesicles. *J. Cell Biol.* **149**, 379–396 (2000).
4. Barbosa, J., Jr. *et al.* Trafficking of the vesicular acetylcholine transporter in SN56 cells: a dynamin-sensitive step and interaction with the AP-2 adaptor complex. *J. Neurochem.* **82**, 1221–1228 (2002).
5. Voglmaier, S.M. *et al.* Distinct endocytic pathways control the rate and extent of synaptic vesicle protein recycling. *Neuron* **51**, 71–84 (2006).
6. De Gois, S. *et al.* Identification of endophilins 1 and 3 as selective binding partners for VGLUT1 and their co-localization in neocortical glutamatergic synapses: implications for vesicular glutamate transporter trafficking and excitatory vesicle formation. *Cell. Mol. Neurobiol.* **26**, 679–693 (2006).
7. Vinatier, J. *et al.* Interaction between the vesicular glutamate transporter type 1 and endophilin A1, a protein essential for endocytosis. *J. Neurochem.* **97**, 1111–1125 (2006).
8. Schuske, K., Beg, A.A. & Jorgensen, E.M. The GABA nervous system in *C. elegans*. *Trends Neurosci.* **27**, 407–414 (2004).
9. Jin, Y., Hoskins, R. & Horvitz, H.R. Control of type-D GABAergic neuron differentiation by *C. elegans* UNC-30 homeodomain protein. *Nature* **372**, 780–783 (1994).
10. Jin, Y., Jorgensen, E., Hartwieg, E. & Horvitz, H.R. The *Caenorhabditis elegans* gene unc-25 encodes glutamic acid decarboxylase and is required for synaptic transmission but not synaptic development. *J. Neurosci.* **19**, 539–548 (1999).
11. McIntire, S.L., Reimer, R.J., Schuske, K., Edwards, R.H. & Jorgensen, E.M. Identification and characterization of the vesicular GABA transporter. *Nature* **389**, 870–876 (1997).
12. Bamber, B.A., Beg, A.A., Twyman, R.E. & Jorgensen, E.M. The *Caenorhabditis elegans* unc-49 locus encodes multiple subunits of a heteromultimeric GABA receptor. *J. Neurosci.* **19**, 5348–5359 (1999).
13. McIntire, S.L., Jorgensen, E. & Horvitz, H.R. Genes required for GABA function in *Caenorhabditis elegans*. *Nature* **364**, 334–337 (1993).
14. Eskelinen, E.L., Tanaka, Y. & Saftig, P. At the acidic edge: emerging functions for lysosomal membrane proteins. *Trends Cell Biol.* **13**, 137–145 (2003).
15. Kostich, M., Fire, A. & Fambrough, D.M. Identification and molecular-genetic characterization of a LAMP/CD68-like protein from *Caenorhabditis elegans*. *J. Cell Sci.* **113**, 2595–2606 (2000).
16. David, A. *et al.* BAD-LAMP defines a subset of early endocytic organelles in subpopulations of cortical projection neurons. *J. Cell Sci.* **120**, 353–365 (2007).
17. Su, A.I. *et al.* Large-scale analysis of the human and mouse transcriptomes. *Proc. Natl. Acad. Sci. USA* **99**, 4465–4470 (2002).
18. Lein, E.S. *et al.* Genome-wide atlas of gene expression in the adult mouse brain. *Nature* **445**, 168–176 (2007).
19. Shan, G., Kim, K., Li, C. & Walthall, W.W. Convergent genetic programs regulate similarities and differences between related motor neuron classes in *Caenorhabditis elegans*. *Dev. Biol.* **280**, 494–503 (2005).
20. Eastman, C., Horvitz, H.R. & Jin, Y. Coordinated transcriptional regulation of the *unc-25* glutamic acid decarboxylase and the *unc-47* GABA vesicular transporter by the *Caenorhabditis elegans* UNC-30 homeodomain protein. *J. Neurosci.* **19**, 6225–6234 (1999).
21. Nonet, M.L. Visualization of synaptic specializations in live *C. elegans* with synaptic vesicle protein-GFP fusions. *J. Neurosci. Methods* **89**, 33–40 (1999).
22. Jorgensen, E.M. *et al.* Defective recycling of synaptic vesicles in synaptotagmin mutants of *Caenorhabditis elegans*. *Nature* **378**, 196–199 (1995).
23. Fremeau, R.T., Jr. *et al.* Vesicular glutamate transporters 1 and 2 target to functionally distinct synaptic release sites. *Science* **304**, 1815–1819 (2004).
24. Richmond, J.E. & Jorgensen, E.M. One GABA and two acetylcholine receptors function at the *C. elegans* neuromuscular junction. *Nat. Neurosci.* **2**, 791–797 (1999).
25. Marsh, M. *et al.* Rapid analytical and preparative isolation of functional endosomes by free flow electrophoresis. *J. Cell Biol.* **104**, 875–886 (1987).
26. Eskelinen, E.L. *et al.* Disturbed cholesterol traffic but normal proteolytic function in LAMP-1/LAMP-2 double-deficient fibroblasts. *Mol. Biol. Cell* **15**, 3132–3145 (2004).
27. Eskelinen, E.L. Roles of LAMP-1 and LAMP-2 in lysosome biogenesis and autophagy. *Mol. Aspects Med.* **27**, 495–502 (2006).
28. Eskelinen, E.L. *et al.* Role of LAMP-2 in lysosome biogenesis and autophagy. *Mol. Biol. Cell* **13**, 3355–3368 (2002).
29. Fukuda, M. Lysosomal membrane glycoproteins. Structure, biosynthesis, and intracellular trafficking. *J. Biol. Chem.* **266**, 21327–21330 (1991).
30. Daniels, R.W. *et al.* A single vesicular glutamate transporter is sufficient to fill a synaptic vesicle. *Neuron* **49**, 11–16 (2006).
31. Harris, T.W., Hartwieg, E., Horvitz, H.R. & Jorgensen, E.M. Mutations in synaptojanin disrupt synaptic vesicle recycling. *J. Cell Biol.* **150**, 589–600 (2000).
32. Nonet, M.L. *et al.* UNC-11, a *Caenorhabditis elegans* AP180 homologue, regulates the size and protein composition of synaptic vesicles. *Mol. Biol. Cell* **10**, 2343–2360 (1999).
33. Schuske, K.R. *et al.* Endophilin is required for synaptic vesicle endocytosis by localizing synaptojanin. *Neuron* **40**, 749–762 (2003).
34. Clark, S.G., Lu, X. & Horvitz, H.R. The *Caenorhabditis elegans* locus *lin-15*, a negative regulator of a tyrosine kinase signaling pathway, encodes two different proteins. *Genetics* **137**, 987–997 (1994).
35. Richmond, J.E., Davis, W.S. & Jorgensen, E.M. UNC-13 is required for synaptic vesicle fusion in *C. elegans*. *Nat. Neurosci.* **2**, 959–964 (1999).
36. Weimer, R.M. *et al.* UNC-13 and UNC-10/rim localize synaptic vesicles to specific membrane domains. *J. Neurosci.* **26**, 8040–8047 (2006).
37. Thompson, J.D., Gibson, T.J., Plewniak, F., Jeanmougin, F. & Higgins, D.I. The ClustalX windows interface: flexible strategies for multiple sequence alignment aided by qualitiy analysis tools. *Nucleic Acids Res.* **25**, 4876–4882 (1997).